CoA Memo. No. 179

February, 1969

THE COLLEGE OF AERONAUTICS

DEPARTMENT OF MATERIALS

Preliminary studies of the time-dependent shear and uniaxial tensile behaviour of oriented polymers

- by -

D. Clayton

List of Contents

List of Symbols

x_1, x_2, x_3	a right hand set of mutually orthogonal co-ordinate axes, where x_3 is in the direction of draw.
i,j	dummy suffices where $i,j = 1,2,3$
w	sample width
t	sample thickness
T	applied torque
α	angle of twist per unit length
Θ	angular deflection
σ	applied stress
E_θ and $E_\theta(t)$	the tensile modulus of a strip cut at $\theta°$ to the draw direction
E_o and $E_o(t)$	the tensile modulus of a strip cut at 0° to the draw direction
E_{90} and $E_{90}(t)$	the tensile modulus of a strip cut at 90° to the draw direction
E_{45} and $E_{45}(t)$	the tensile modulus of a strip cut at 45° to the draw direction
S_{ij} and $S_{ij}(t)$	the matrix of compliances
S_{33} and $S_{33}(t)$	the tensile compliance of a strip cut at 0° to the draw direction
S_{11} and $S_{11}(t)$	the tensile compliance of a strip cut at 90° to the draw direction
S_{13} and $S_{13}(t)$	the contraction compliance of a strip cut at 0° to the draw direction
S_{12} and $S_{12}(t)$	the contraction compliance of a strip cut at 90° to the draw direction
S_{44} and $S_{44}(t)$	the shear compliance governing laminar shear in the 1-3 and 2-3 planes.
S_{66} and $S_{66}(t)$	the shear compliance governing laminar shear in the 1-2 plane.

ν_{13} and $\nu_{13}(t)$	the creep contraction ratio of a strip cut at 0° to the draw direction
ν_{12} and $\nu_{12}(t)$	the creep contraction ratio of a strip cut at 90° to the draw direction
$\nu_{(\theta°)}$	the creep contraction ratio of a strip cut at θ° to the draw direction
$\nu_{(45°)}$ and $\nu_{(45°)}(t)$	the creep contraction ratio of a strip cut at 45° to the draw direction
$\epsilon_{33}(t)$	the tensile strain in the 3 direction
$\epsilon_{11}(t)$	the tensile strain in the 1 direction
$\epsilon_{12}(t)$	the contraction strain in 1 direction due to an applied stress in the 2 direction
$\epsilon_{13}(t)$	the contraction strain in 1 direction due to an applied stress in the 3 direction.
$T^{\epsilon}(45°)(t)$	the tensile strain in the direction of the applied stress for a specimen cut at 45° to the draw direction
$C^{\epsilon}(45°)(t)$	the contraction strain in a direction transverse to the applied stress for a specimen cut at 45° to the draw direction.

List of figures

Fig. 6.11 The variation of the measured and calculated 100 second shear compliance, $S_{44}(t)$ with draw ratio.

Fig. 6.12 The variation of the 100 second creep modulii $E_o(t)$, $E_{90}(t)$ and $E_{45}(t)$ with draw ratio at 1% 100 second strain.

Fig. 6.13 The variation of the 100 second contraction compliance $S_{12}(t)$ and $S_{13}(t)$, with draw ratio at 1% 100 second strain.

Fig. 6.14 The variation of the 100 second creep contraction ratio, $\nu_{12}(t)$ and $\nu_{13}(t)$, with draw ratio at 1% 100 second strain.

Fig. 6.15 The variation of the measured and calculated 100 second creep contraction ratio, $\nu_{(45°)}(t)$, with draw ratio at 1% 100 second strain.

Fig. 6.16 The variation of the 100 second shear compliance, $S_{66}(t)$ with draw ratio at 1% 100 second strain.

Fig. 6.17 The variation of the 100 second creep modulus, $E_{90}(t)$, with 100 second tensile strain, $\epsilon_{11}(t)$, for different draw ratios.

Fig. 6.18 The variation of the 100 second creep modulus, $E_o(t)$, with 100 second tensile strain, $\epsilon_{33}(t)$, for different draw ratios.

Fig. 6.19 The variation of the 100 second creep modulus, $E_{45}(t)$, with 100 second tensile strain $T^{\epsilon}{}_{(45°)}(t)$, for different draw ratios.

Fig. 6.20 The variation of the 100 second contraction compliance, $S_{12}(t)$, with 100 second tensile strain, $\epsilon_{11}(t)$, for different draw ratios.

Fig. 6.21 The variation of the 100 second contraction compliance $S_{13}(t)$ with 100 second tensile strain, $\epsilon_{33}(t)$, for different draw ratios.

Fig. 6.22 The variation of the 100 second creep contraction ratio $\nu_{12}(t)$, with 100 second tensile strain, $\epsilon_{11}(t)$, at different draw ratios.

Fig. 6.23 The variation of the 100 second creep contraction ratio $\nu_{13}(t)$ with 100 second tensile strain, $\epsilon_{33}(t)$ at different draw ratios.

Fig. 6.24 The variation of the 100 second creep contraction ratio $\nu_{(45°)}(t)$ with 100 second tensile strain, $T^{\epsilon}{}_{(45°)}(t)$, for different draw ratios.

Fig. 6.25 The variation of the rate of change of tensile compliance, $\frac{d(S_{11}(t))}{d \log t}$, with log (time) for different draw ratios.

Fig. 6.26 The variation of the rate of change of tensile compliance, $\frac{d(S_{33}(t))}{d \log(t)}$, with log (time) for different draw ratios.

Fig. 6.27 The variation of the rate of change of tensile compliance, $\frac{d(\frac{1}{E_{45}(t)})}{d \log t}$, with log (time) for different draw ratios.

Fig. 6.28 The variation of the rate of change of shear compliance, $\frac{d(S_{44}(t))}{d \log t}$, with log (time) for different draw ratios.

1. Summary

The work reported in this memo is the initial stages of an investigation of the time-dependent behaviour of certain anisotropic polymers. In the first instance low density polyethylene with a transversely isotropic symmetry is being examined. Different degrees of anisotropy have been induced by cold drawing and the time dependent material parameters necessary to describe the stiffness of the anisotropic polyethylene have been determined. This involved the measurement of uniaxial tensile creep, lateral contraction creep, and torsional creep under conditions of constant load at 20°C ± 0.5°C.

The tensile creep and contraction creep apparatus has been described elsewhere (Darlington (a) 1968) and only the principle of the apparatus is discussed here. The torsional creep apparatus is described in detail. Analysis of the experimental data is not yet complete. The data is tabulated in section 5 and a preliminary analysis is presented in section 6.

Details of proposed future work are discussed in section 7.

2. Introduction

The mechanical properties of an isotropic elastic material are defined when two of the material constants i.e. Young's Modulus, E, Poisson's ratio, ν, Shear Modulus, G, and Bulk Modulus, K, are known. For most engineering applications the temperature coefficient of these quantities may be ignored and the elastic constants may be regarded as temperature independent. However, polymeric materials exhibit ma rked time and temperature dependence and it is not a simple matter to describe their mechanical behaviour. A full description involves relaxation times over a range of 20 decades of time. To describe the mechanical properties of an isotropic linear viscoelastic material the variation of the tensile compliance $S_{11}(t)$ and shear compliance $S_{44}(t)$ with time and temperature are needed. In the past few years the major polymer producers have published a large amount of information on the mechanical properties of plastics. The majority of the data has been obtained from uniaxial tensile creep experiments on isotropic materials and is used by the engineer when considering the time-dependent behaviour of a plastics component. However, components manufactured from polymeric materials by the usual processing techniques are frequently anisotropic. Thus, the mechanical properties vary with direction and consequently the behaviour of the component in service becomes more difficult to predict. One aim of the present investigation, and future work, is to examine the mechanical properties of a number of polymers in which a controlled anisotropy has been induced. The first investigations are being carried out using a low density polyethylene which has been cold drawn into a state of transverse isotropy, the plane of isotropy being perpendicular to the draw direction. The degree of anisotropy will depend on how much the polymer is drawn, and the Draw Ratio, defined as the ratio of the final length of a line in the direction of draw to the initial length

is a convenient measure of anisotropy (Rauman and Saunders, 1961). To describe the mechanical properties of a transversely isotropic linear visco-elastic material the necessary measurements are those of tensile compliances $S_{11}(t)$ and $S_{33}(t)$, the contraction compliances $S_{12}(t)$ and $S_{13}(t)$, and the shear compliance $S_{44}(t)$. Clearly an investigation of this type over 20 decades of time is impractical and it is more usual to use a measuring technique which covers several decades of time and to vary the temperature of the experiment. The compliances $S_{11}(t)$, $S_{33}(t)$, $S_{12}(t)$ and $S_{13}(t)$, have been measured in a uniaxial tensile and transverse contraction creep experiment at times between 5 and 1000 seconds at 20°C ± 0.5°C. The shear compliance $S_{44}(t)$ has been measured for times between 5 and 2000 seconds using a torsional creep apparatus. The apparatus has also been instrumented to perform forced oscillation experiments up to 2Hz. For higher frequencies a torsion pendulum has been built which can operate at frequencies between 0.1 Hz and 10 Hz. The torsional creep apparatus and torsion pendulum can easily be modified to include a temperature enclosure and it is intended to use the equipment at a series of controlled temperatures between - 180°C and room temperature in the near future.

The long term creep measurements have so far been limited to a strain range for which the material behaves in an approximately linear viscoelastic manner. It is intended in future work to study the long term behaviour in the non-linear region.

For the analysis of the data presented in section 6 it has been assumed that the compliance matrix describing the mechanical properties of the material has a form analogous to that of the equivalent transversely isotropic elastic material. Strain energy considerations show that for an elastic material $S_{ij} = S_{ji}$ and hence there are 5 independent compliance parameters. We shall assume the corresponding relationships $S_{ij}(t) = S_{ji}(t)$ for the visco-elastic material. The validity of these relationships has been discussed by, for example, Biot (Biot, 1954). The time dependent compliance matrix then takes the form:-

$$S_{ij}(t) = \begin{pmatrix} S_{11}(t) & S_{12}(t) & S_{13}(t) & & & \\ & S_{11}(t) & S_{13}(t) & & & \\ & & S_{33}(t) & & & \\ & & & S_{44}(t) & & \\ & & & & S_{44}(t) & \\ & & & & & S_{66}(t) \end{pmatrix} \qquad (2.1$$

where x_1, x_2, x_3 are a right hand set of mutually orthogonal co-ordinate axes,

and x_3 is perpendicula r to the plane of isotropy in the direction of draw.

and where $S_{11}(t)$, $S_{33}(t)$, are the tensile creep compliances

$S_{12}(t)$, $S_{13}(t)$ are the creep contraction compliances

and $S_{44}(t)$, $S_{66}(t)$ are the shear creep compliances also from symmetry considerations:-

$$S_{66}(t) = 2[S_{11}(t) - S_{12}(t)] \tag{2.2}$$

Again following Classical Elasticity Theory, the Young's Modulus, E_θ, i.e. the modulus of a strip cut in the plane of the sheet at an angle θ to the symmetry direction, is given by

$$\frac{1}{E_\theta} = S_{33}\cos^4\theta + (2S_{13} + S_{44})\sin^2\theta\cos^2\theta + S_{11}\sin^4\theta \tag{2.3}$$

thus by putting $\theta = 0°$ $^1/E_o = S_{33}$, $\theta = 90°$ $^1/E_{90} = S_{11}$ and by putting $\theta = 45°$

$$\frac{4}{E_{45}} = S_{33} + (2S_{13} + S_{44}) + S_{11} \tag{2.4}$$

or
$$S_{44} = \frac{4}{E_{45}} - S_{33} - S_{11} - 2S_{13} \tag{2.5}$$

Hence by taking measurements of $E_{45}(t)$, and knowing $S_{33}(t)$, $S_{11}(t)$, $S_{13}(t)$ an estimate of $S_{44}(t)$ may be made by assuming the above relationship (2.5) holds for a visco-elastic material viz:

$$S_{44}(t) = \frac{4}{E_{45}(t)} - S_{33}(t) - S_{11}(t) - 2S_{13}(t) \tag{2.6}$$

The compliance $S_{11}(t)$, $S_{12}(t)$ are calculated from readings of uniaxial extension and transverse contraction in a uniaxial tensile creep test on a specimen cut at 90° to the draw direction. The compliance $S_{11}(t)$ is the ratio of the time dependent creep strain $\epsilon_{11}(t)$ to the applied stress viz.

$$S_{11}(t) = \frac{\epsilon_{11}(t)}{\sigma} \tag{2.7}$$

and the compliance $S_{12}(t)$ is the ratio of the time dependent contraction strain $\epsilon_{12}(t)$ to the applied stress viz.

$$S_{12}(t) = \frac{\epsilon_{12}(t)}{\sigma} \tag{2.8}$$

Similarly $S_{33}(t)$ and $S_{13}(t)$ are obtained from corresponding measurements on a sample cut at 0° to the draw direction, and $E_{45}(t)$ from a sample cut at 45° to the draw direction. Thus:-

$$S_{33}(t) = \frac{\epsilon_{33}(t)}{\sigma} \tag{2.9}$$

$$S_{13}(t) = \frac{\epsilon_{13}(t)}{\sigma} \tag{2.10}$$

and $$E_{45}(t) = \frac{\epsilon_{(45°)}(t)}{\sigma} \tag{2.11}$$

The transverse contraction of a 45° sample was measured at three selected draw ratios. From the Classical Theory of Elasticity it can be shown that for a sample cut at $\theta°$ to the draw direction, the contraction ratio, $\nu_{(\theta°)}$ is given by:-

$$\nu_{(\theta°)} = -\left(\frac{S_{13}\cos^2\theta + S_{12}\sin^2\theta}{S_{33}\cos^4\theta + (2S_{13} + S_{44})\sin^2\theta\cos^2\theta + S_{11}\sin^4\theta}\right) \tag{2.12}$$

or in particular at 4 5° is given by:-

$$\nu_{(45°)} = -2\left(\frac{S_{13} + S_{12}}{S_{33} + (2S_{13} + S_{44}) + S_{11}}\right) \tag{2.13}$$

Thus, by comparing the measured and calculated creep contraction ratio $\nu_{(45°)}(t)$ it is possible to assess the usefulness of the equations of Classical Elasticity when applied to a visco-elastic material.

The above tensile measurements were taken on an apparatus designed by Darlington (Darlington, 1968), the principle of which is briefly described in section 4.

The shear compliances $S_{44}(t)$ and $S_{66}(t)$ are calculated from readings of angular deflection, Θ, and applied torque, T, in a torsional creep experiment where the torsion axis is along the direction of draw, and at 90° to the direction of draw, respectively. The compliance, $S_{44}(t)$ may be found directly from a torsion experiment about the draw direction, as this compliance governs the laminar shear in the 3,1 and 3,2 planes. Again applying the results of Classical Elasticity Theory to the visco-elastic case we have

$$S_{44}(t) = \frac{\alpha}{T}\frac{\omega t^3}{16}\left[\frac{16}{3} - \frac{t}{\omega}\left(\frac{4}{\pi}\right)^5\right] \tag{2.14}$$

for $\omega \geq 3t$

where α is the angle of twist per unit length

$$\text{i.e. } \alpha = \frac{\Theta}{L} \tag{2.15}$$

and T is the applied torque.

However, by testing a sample at 90° to the draw direction the laminar shear in the 3,2 plane is governed by $S_{44}(t)$, and in the 1,2 plane by $S_{66}(t)$. Thus $S_{66}(t)$ cannot be found directly and the values of $S_{44}(t)$ under the same conditions of time and temperature must be known. For $S_{66}(t)$ to be the dominant compliance necessitates a sample which in practice is difficult to obtain, since this involves cutting a sample whose width is the through thickness of the draw sheet. Following Classical Elasticity Theory the expression for $S_{66}(t)$ is given by:-

$$S_{66}(t) = \frac{\alpha}{T} \cdot \frac{\omega t^3}{16}\left[\frac{16}{3} - \frac{t}{\omega}\left(\frac{S_{44}(t)}{S_{66}(t)}\right)^{\frac{1}{2}} \cdot \left(\frac{4}{\pi}\right)^5 \tanh\left\{\frac{\pi}{2}\frac{\omega}{t}\left(\frac{S_{66}(t)}{S_{44}(t)}\right)^{\frac{1}{2}}\right\}\right] \tag{2.16}$$

where $\alpha = \Theta/L$ and T is the applied torque.

Mainly due to the practical difficulties, but also due to the complexity of (2.16) the compliance $S_{66}(t)$ will only be measured at two or three draw ratios, and the other values of $S_{66}(t)$ will be calculated using (2.2).

Another feature of the work is the interpretation of the properties in terms of mechanisms which may describe the deformation processes in the material. Recently Darlington (Darlington, b, 1968) and Hinton (Hinton, 1968) have discussed the possibility of a 'slip' or 'easy-shear' mechanism which is responsible for the material deformation, the 'slip' occurring on planes perpendicula r to the plane of the sheet and parallel to the draw direction. Darlington has worked on highly drawn low density polyethylene at strains between 0.1% and 10%, whereas Hinton has worked on highly drawn polyethylene at or near their Yield Points. Both sets of work indicate the possibility of an 'easy-shear' mechanism which dominates the deformation process from low strains up to Yield in highly drawn polyethylene. The work reported here, and the work proposed for the near future, has been on a low density polyethylene at a variety of draw ratios from the isotropic state to the highly drawn (draw ratio around 3.8), at strains up to 5%. It is hoped that results may be forwarded which will support, or counter, the work of Darlington and Hinton. The results will be examined to see if Darlington's easy shear model is a feasible deformation processes and also to see if this is the dominant process at the lower draw ratios.

3. Sample Preparation and Characterisation.

3.1 Preparation of the Isotropic Sheets

The grade of polyethylene chosen was I.C.I. 'Alkathene' W.J.G.11. It was obtained in the form of cube granules and isotropic sheets were prepared by compression moulding the granules between highly polished aluminium plates at 160°C. Thin sheets of polyethylene teraphthalate, 'Melinex', were used between the polymer and the plates to avoid adhesion problems when removing the pressed polymer sheets. The molten polymer was held in the press at 160°C for 15 minutes before rapidly cooling by passing cold water through the press. The heating period was necessary to remove strains caused by the flow pattern of the polymer during pressing. The isotropic sheets have a nominal thickness of 0.166 cms. The mechanical isotropy of the sheets was checked by measuring the yield stress for samples cut at various angles and positions in several sheets. No systematic variation with angle or position could be detected. The value of yield stress was 1300 lbf/in^2 at a temperature of 25°C for constant extension rate. This value was in agreement with Darlington (1966) who reported the properties of a similar isotropic sheet prepared in the same manner. Darlington measured the density of the isotropic sheet from 20 hours to 500 hours after preparation and found that a steady value was not attained. The variation was small however being less than 0.0004 grm/cc. The mean density was 0.917 grm/cc. which corresponds to a crystallinity of approximately 47%.

3.2 Preparation and Characterisation of the Draw Samples

After the isotropic sheets had been in storage for a period of 12 to 15 days, anisotropic sheets were prepared by selecting uniform isotropic sheets of length 15 to 24 cms, and width 6 to 8 cms, and cold drawing in uniaxial tension. A grid of half centimetre squares marked on each sheet prior to the drawing process was used in the determination of the final draw ratio. The drawn sheets were stored for 3 to 4 weeks at room temperature (21°C) before samples were taken.

4. Apparatus

4.1 The Tensile Creep and Transverse Contraction Apparatus

A detailed description of the apparatus and the extensometry has been given by Darlington (Darlington, a, 1968), and a schematic diagram is shown in figure 4.1.

The specimen is loaded via the lever loading system and the slide guide. The slide guide ensures that the load is applied axially and also that the specimen is free from any transverse or torsional loading. The loads are applied in a steady manner in about 0.5 to 1 second.

The tensile creep extension and transverse creep contraction are monitored

simultaneously by extensometers 1 and 2 respectively. The transducers and recording apparatus can detect deflections down to 5×10^{-6} on a gauge length of only 0.5 inches.

On an individual specimen the machine accuracy is better than 1%, but the largest error arises due to inter-specimen reproducibility and an accracy of ± 2% is claimed on a tensile compliance and ± 3% on the contraction data.

4.2 The Torsional Creep Apparatus

The torsional creep apparatus is based on an early design by Morrison et al (1955) and is shown schematically in Fig 4.2a. The coil consists of 1300 turns of 40 SWG enamelled copper wire suspended in the field of a Magnetron permanent magnet by a 0.015" suspension wire. The upper sample clamp is attached to the coil and by applying a voltage across the coil torques up to 3000 gm. cm. may be applied to a sample. The pole pieces have been machined so that the torque is directly proportional to the applied voltage and independent of the angular deflection over the range of deflections encountered. Thus the torque applied to the sample remains constant during a creep exper iment. To test the linearity of the field the deflection of a metal shim was noted for a given applied voltage. The magnetic field was then rotated and the test repeated, for the same applied voltage the deflection remained constant. The applied voltage is continuously displayed on a Digital Voltmeter and over the range of times used the voltage fluctuations are around 0.1%. The bottom clamp is firmly attached to a linear bearing. This device restricts all rotational movement of the clamp but allows almost free axial movement. Thus specimens of varying length may be mounted in the apparatus and also thermal expansion and contraction may occur freely without applying extraneous axial loads to the specimen. Another feature of the bearing is that selected axial loads may be applied to the specimen thus enabling combined tensile and torsional creep experiments.

The instrumentation used for the load application is shown in Fig. 4.2b. The Farnell stabilised voltage supply (S.V.S.1) drives a linear potentiometer via a motor and gear box. The potentiometer replaces the control knob on the second stabilised voltage supply (S.V.S.2) and the two cams (C1, C2) and associated micro switches (Ms.1 and Ms.2) control the extent of the rotation of the potentiometer and thus the voltage supplied to the coil. The time of application of the load can be varied from a fraction of a second to several seconds and this facility will be used in future work to apply ramp function inputs which with suitable analysis can yield the compliance at times less than 5 seconds.

In another arrangement (dotted lines) the motor and gearbox can drive a sine- cosine potentiometer (S/C pot). A constant voltage is supplied to the input terminals of the sine-cosine potentiometer and a sinusoidal voltage output is fed to the coil. The peak to peak voltage is determined by the input voltage and the frequency by the speed of the motor. Frequencies

usually encountered are in the region of 0.003 Hz to 2 Hz.

The angular deflections are measured using an optical lever system. The reflected light spot is automatically followed by the photocell in a Graphis pot recorder. The deflections are read to 1 mm. which with the present optical lever is equivalent to an angular deflection of approximately 2 minutes of arc.

The instrument is calibrated such that the torque applied is known in terms of the voltage drop across the coil which is read on a Digital Voltmeter reading to 0.1%.

4.3 The Torsion Pendulum

The apparatus is an inverted torsion pendulum designed to investigate the dynamic mechanical properties of polymers using free-damped oscillations. A schematic representation of the apparatus is given in fig. 4.3

The bottom specimen clamp is rigidly fixed to a linear bearing of the type used in the torsional creep apparatus. The upper clamp forms part of the inertia system, the remainder of which consists of an aluminium boss, two horizontal inertia bars and two inertia bobs when necessary. The inertia bars have been machined with a micro-thread so that the inertia bobs may be screwed to the same radial distance from the axis of rotation to better than 0.001". The inertia of the system is varied either using bars of different materials and addition of inertia bobs or by varying the position of the bobs on the bars.

The inertia system is suspended from a phosphor bronze suspension element attached to the upper fixed plate by a ground and polished slide guide and mateing bush. Preliminary experiments had shown that the use of relatively flexible samples such as low density polyethylene in conjunction with a wire suspension had led to unwanted ancillary vibrations in the system which appeared as perturbations in the desired torsional vibrations. A special suspension system with a cruciform cross-section was designed to be weak in torsion but stiff in flexure and thus stray vibrations were eliminated.

The system has been carefully machined and constructed so that the axis of symmetry of the system and sample is coincident with the axis of rotation. Thus only a pure torsional vibration is imparted to the system.

Different length samples can be accommodated by adjusting the position of the slide guide in the bush.

A mirror attached to the suspension element reflects a beam of light onto the photo-cell of a Graphis pot chart recorder. The photo-cell is seated on the pen carriage of the instrument and automatically follows the light spot so that a trace of the oscillations is recorded on the chart. The chart speeds are from 0.6 mm/min. to 600 mm/min. The frequency and the logarithmic decrement of the oscillations are determined from the chart knowing

the chart speed. The frequency is determined to 0.1% and logarithmic decrement to about 1%.

The system is set in oscillation by two electro-magnets set symmetrically about the torsion axis.

5. Results

Tables 1-18 are the resu lts of the tests on specimens cut at 0° to the draw direction at draw ratios, 1.05, 1.15, 1.20, 2.65, and 3.8. A series of tests were performed at each draw ratio at different stress levels and the applied load is indicated in each case. The readings of time and corresponding deflection at each stress level are tabulated for the creep and recovery experiment. The compliances $S_{33}(t)$ and $S_{13}(t)$ are calculated from equations (2.9) and (2.10) where:-

$$\epsilon_{33}(t) = \left(\frac{\text{Tensile Creep Deflection}}{\text{Gauge Length}}\right) \Big/ \text{applied stress} \qquad (5.1)$$

and

$$\epsilon_{13}(t) = \left(\frac{\text{Contraction Deflection}}{\text{Thickness}}\right) \Big/ \text{applied stress} \qquad (5.2)$$

Similarly Tables 19-42 and Tables 43-55 show the results of the tests on specimens cut at 90° and 45° to the draw direction, respectively, over the same range of draw ratios. Again each sample was tested at different stress levels. The compliances, $S_{11}(t)$, $S_{12}(t)$ and $\frac{1}{E_{45}(t)}$ are calculated from equations (2.7) and (2.8) and (2.11) where

$$\epsilon_{11}(t) \text{ and } \epsilon_{(45°)} = \left(\frac{\text{Tensile Creep Deflection}}{\text{Gauge Length}}\right) \Big/ \text{applied stress} \qquad (5.3)$$

and

$$S_{12}(t) = \left(\frac{\text{Contraction Deflection}}{\text{Thickness}}\right) \Big/ \text{applied stress} \qquad (5.4)$$

The creep contraction ratios $\nu_{13}(t)$, $\nu_{12}(t)$, and $\nu_{(45°)}(t)$ are calculated from the ratio of the lateral contraction strain to the uniaxial tensile strain on specimens cut at 0°, 90°, and 45° to the draw direction respectively. Thus we have:-

$$\nu_{13}(t) = \frac{\epsilon_{13}(t)}{\epsilon_{33}(t)} \qquad (5.5)$$

$$\nu_{12}(t) = \frac{\epsilon_{12}(t)}{\epsilon_{11}(t)} \qquad (5.6)$$

and $$\nu_{(45°)}(t) = \frac{\text{lateral contraction strain of a } 45° \text{ sample}}{\text{uniaxial tensile strain of a } 45° \text{ sample}}$$

$$= \frac{C^{\epsilon}(45°)(t)}{T^{\epsilon}(45°)(t)} \qquad (5.7)$$

6. Analysis and Discussion of Results

As this is only an interim report only a brief description of the results will be given and a more detailed analysis will be presented at a later date when other samples have been tested and the results fully analysed. The plotted results of compliance as a function of time have been selected from the tests where the creep times were up to 1000 seconds. At intermediate stress levels tests were only continued for times up to 100 seconds. The results of the tests in the region where the material is non-linear are tabulated but have not been analysed. Recovery data is also available for all tests but has not yet been analysed. In general the long term data was taken in tests where the uniaxial strain after 100 seconds was around 0.5% and 1% respectively. In the torsional creep tests the maximum surface strains were around 0.1%.

The analysed data is presented in graphical form in figures 6.1 to 6.28. Figures 6.1 to 6.5 show the variation of the compliances with time at different draw ratios as calculated from equations 2.7 - 2.10. Clearly the highly drawn specimens are le ss time dependent than those at the lower draw ratios, and the effect of increased draw ratio has a marked effect on the magnitude of the compliance. The tensile measurements are shown at two different 100 second tensile strains nominally 0.5% and 1%. Whilst there is no marked difference of the time dependence with strain, at this particular strain level, the magnitude of the compliance is noticeably different.

The creep contraction ratios $\nu_{13}(t)$ and $\nu_{12}(t)$, calculated from equations 5.5 and 5.6, are plotted in Figures 6.6 and 6.7. Note how the ratio increases with increasing time and does not remain constant. In figure 6.7 only the results at three draw ratios have been plotted, as the remaining measurements all fall within the same band as the results shown.

To enable calculated values of the shear compliance $S_{44}(t)$ to be made and also to test the usefulness of equations 2.5 and 2.13, the tensile compliance $\frac{1}{E_{45}(t)}$ and the creep contraction ratio $\nu_{(45°)}(t)$ at a sample cut at 45° to the draw direction was calculated using equations 2.11 and 5.7. The tensile compliance at different 100 second tensile strains and different draw ratios is shown in figure 8, and the contraction results in figure 6.9. Again the creep contraction ratio increases with increasing time.

The difficulties of measuring $S_{66}(t)$ were discussed in section 2, and to date no direct measurements of $S_{66}(t)$ have been achieved, however, values have been calculated from equation 2.2 and these have been plotted in figure 6.10.

The effect of draw ratio on the 100 second values of the compliances at 1% tensile stress is shown in figures 6.11 - 6.13. Figure 6.11 also shows a comparison of the measured shear compliance $S_{44}(t)$ with the values calculated from tensile measurements. Realizing that the calculated values were obtained from four other measurements on three different samples and also that two different pieces of apparatus working in different modes of deformation are involved the closeness of fit is quite encouraging, the largest error being about 10%. One departure from the calculated values is in the range of draw ratio isotropic to 1.2. The tensile results predict an initial fall in compliance followed by an increase with increasing draw ratio. However, this 'blip' was not observed in practice and it is felt that more work is needed in this region.

The variation of creep contraction ratio with draw ratio is shown in figure 6.14 and 6.15 for samples cut at 0°, 90° and 45° to the draw direction. Figure 6.14 shows how even for small degrees of anisotropy the creep contraction ratio can vary considerably. Also the variation of creep contraction ratio with draw ratio is different for the three angles tested. Figure 6.15 also shows a comparison of measured and calculated values of $\nu_{(45°)}(t)$ obtained from equation 2.13.

The variation of the calculated shear compliance $S_{66}(t)$, with draw ratio is shown in figure 6.16. The initial increase in compliance at the low draw ratios has been predicted before by Raumann (Raumann, 1962) and it is felt that this is a true feature of the curve.

The extent of linearity of a material may be examined by studying the variation of modulus with strain. Figures 6.19 - 6.21 present log (compliance) as a function of log (strain) and show the deviations from the straight line parallel to the abscissa which is predicted by a linear visco-elastic material. In general above 1% tensile strain samples at all draw ratios are exhibiting non-linear behaviour. Figures 6.22 - 6.24 show the variation of the 100 second creep contraction ratios with tensile strain.

In order to look at the mechanisms which may be controlling the deformation the rate of change of compliance with time has been calculated as this is a first approximation to the retardation spectrum and the results are shown in figures 6.25 - 6.28. Two mechanisms appear to be present, one for the samples at low draw ratios and one for the highly drawn specimens Further work at intermediate draw ratios is needed and also data obtained at various controlled temperatures before any conclusions can be reached about the mechanisms of deformation.

7. Future Work

The results presented in this memo need complementing by further measurements, these may be itemised as follows:

7.1 The discrepancy between the measured and calculated values of the shear compliance, $S_{44}(t)$ at low draw ratios must be resolved by doing further tests. The necessary samples are now being prepared for this part of the programme.

7.2 The variation of 100 second compliance values with draw ratio (figures 6.11 - 6.15) and the rate of change of compliance with time (figures 6.25 - 6.28) proved extremely interesting and it will be profitable to examine further samples of intermediate draw ratios. The necessary samples are now being prepared.

7.3 To facilitate a non-linear analysis measurements of compliances will be made above 1% tensile strain to longer times. This will necessitate extending the torsional creep measurements to higher strains.

7.4 The difficulty of measuring $S_{66}(t)$, directly has not yet been resolved. However, some $\frac{1}{2}''$ isotropic sheets have been pressed and drawn and it is hoped that samples may be prepared in order to attempt these measurements.

7.5 It appears in figures 6.25 - 6.28 that at times less than 5 seconds the compliances change slope markedly and this may be indicative of a deformation mechanism, thus further investigations at times less than 5 seconds would be extremely useful. This may be done using the torsion pendulum and forced oscillation techniques or by applying a controlled ramp function and measuring the resulting deformation. Results will be taken over a range of temperatures between 20°C and - 180°C. The equipment for the low temperature work has been purchased and only a temperature control unit is needed.

7.6 Work of a more theoretical nature will be continued aimed at an analytical analysis of the data obtained in both the linear and non-linear regions using the anisotropic visco-elastic theories discussed by, for example, Schapery (Schapery, 1967), Rogers (Rogers, et al., 1963), and Findley (Findley et al., 1968).

References

1. Biot, M.A. (1954). J. Appl. Phys. Vol. 25, No. 11, p. 1385, 1954.

2. Darlington, M.W. (1966). College of Aeronautics Memo. No. 115, Oct. 1966.

3. Darlington, M.W. and Saunders, D.W. (a) 1969 - to be published.
(b) 1969 - to be published.

4. Findley, W.N. (1968). Trans. Soc. Rheol. 12:2, p. 217, (1968).

5. Hinton (1968) Private Communication.

6. Raumann, G. and Saunders, D.W. (1961). Proc. Phys. Soc. 77, 1028, (1961).

7. Raumann, G. (1962). Proc. Phys. Soc. 79 1221, (1962).

8. Rogers, T.G. and Pipkin, A.C. (1963). ZAMP, 14, 334 (1963).

9. Schapery, R.A. (1967). J. Comp. Mtls. 1, 228, 1967.

Acknowledgements

I would like to thank my supervisor Dr. M.M. Hall for his encouragement and helpful advice during all stages of the work and for his many useful comments during the preparation of the report.

I acknowledge grateful thanks to Dr. M.W. Darlington for the many invaluable discussions concerning the work and the finer points of creep testing and also for making his tensile creep apparatus available to me.

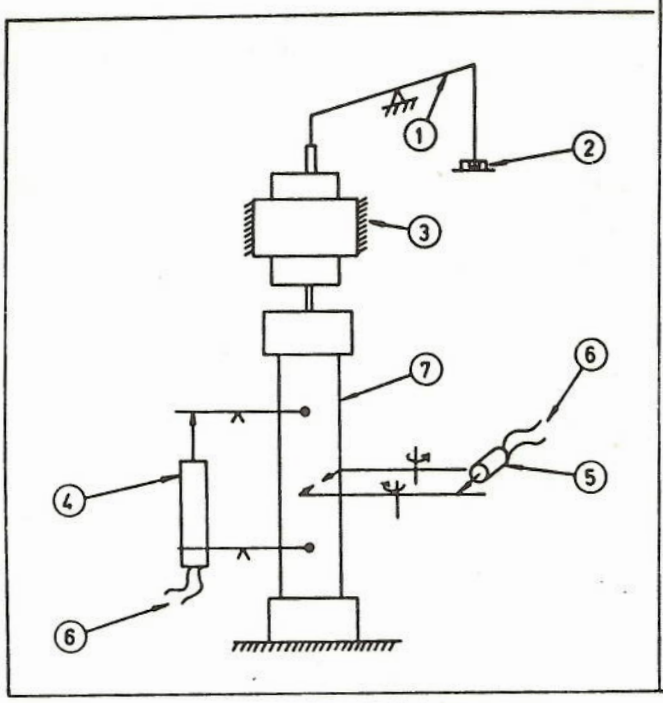

FIGURE 4·1 A SCHEMATIC REPRESENTATION OF THE TENSILE CREEP AND TRANSVERSE CONTRACTION APPARATUS (DARLINGTON 1968)

① THE LEVER LOADING SYSTEM ② APPLIED LOAD
③ SLIDE GUIDE ④ UNIAXIAL CREEP EXTENSOMETER 1.
⑤ CONTRACTION CREEP EXTENSOMETER 2.
⑥ LEADS TO RECORDING APPARATUS. ⑦ SAMPLE

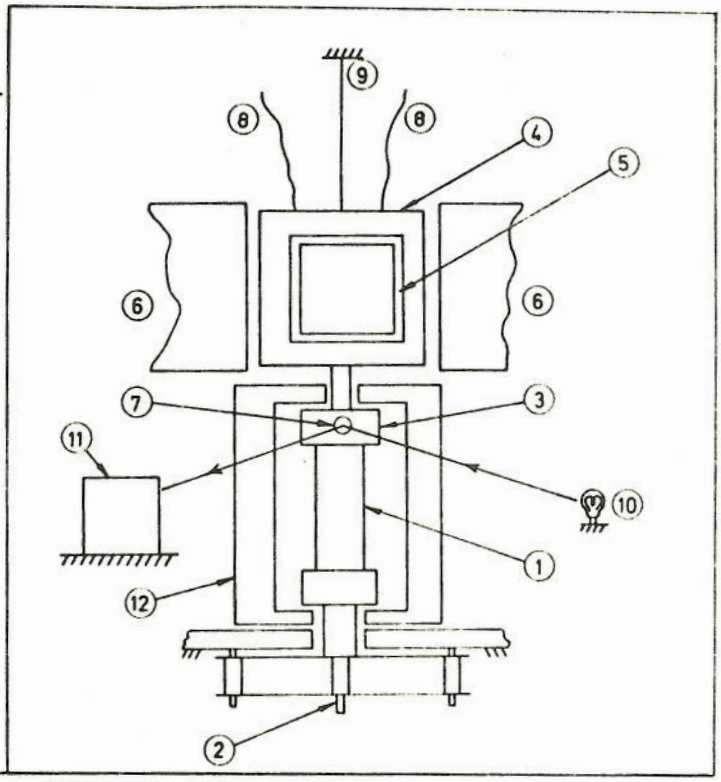

FIGURE 4·2a THE TORSIONAL CREEP APPARATUS

①SAMPLE ②BOTTOM CLAMP AND LINEAR BEARING ARRANGEMENT
③ UPPER CLAMP ④ COIL AND FORMER ⑤ SOFT IRON CORE
⑥ PERMANENT MAGNET ⑦ MIRROR ⑧ INPUT LEADS TO COIL
⑨ FINE SUSPENSION WIRE ⑩ LIGHT SOURCE ⑪ GRAPHISPOT RECORDER ⑫ TEMPERATURE ENCLOSURE.

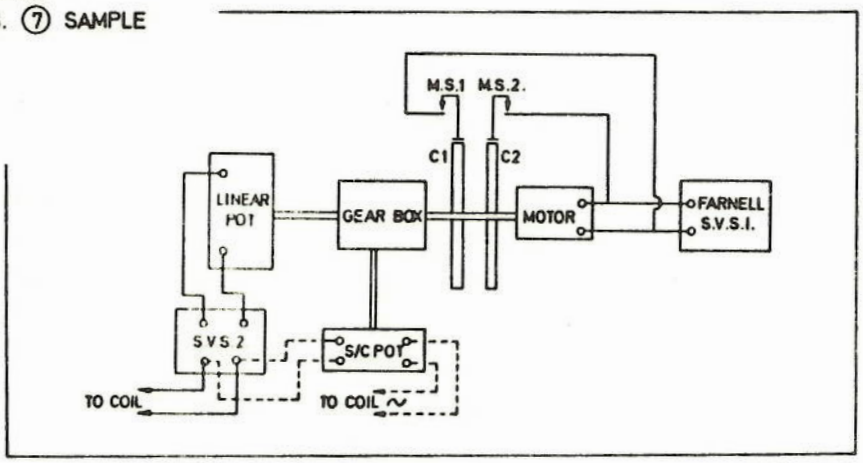

FIGURE 4·2b THE INSTRUMENTATION USED FOR LOAD APPLICATION FOR THE TORSIONAL CREEP AND FORCED OSCILLATION APPARATUS.

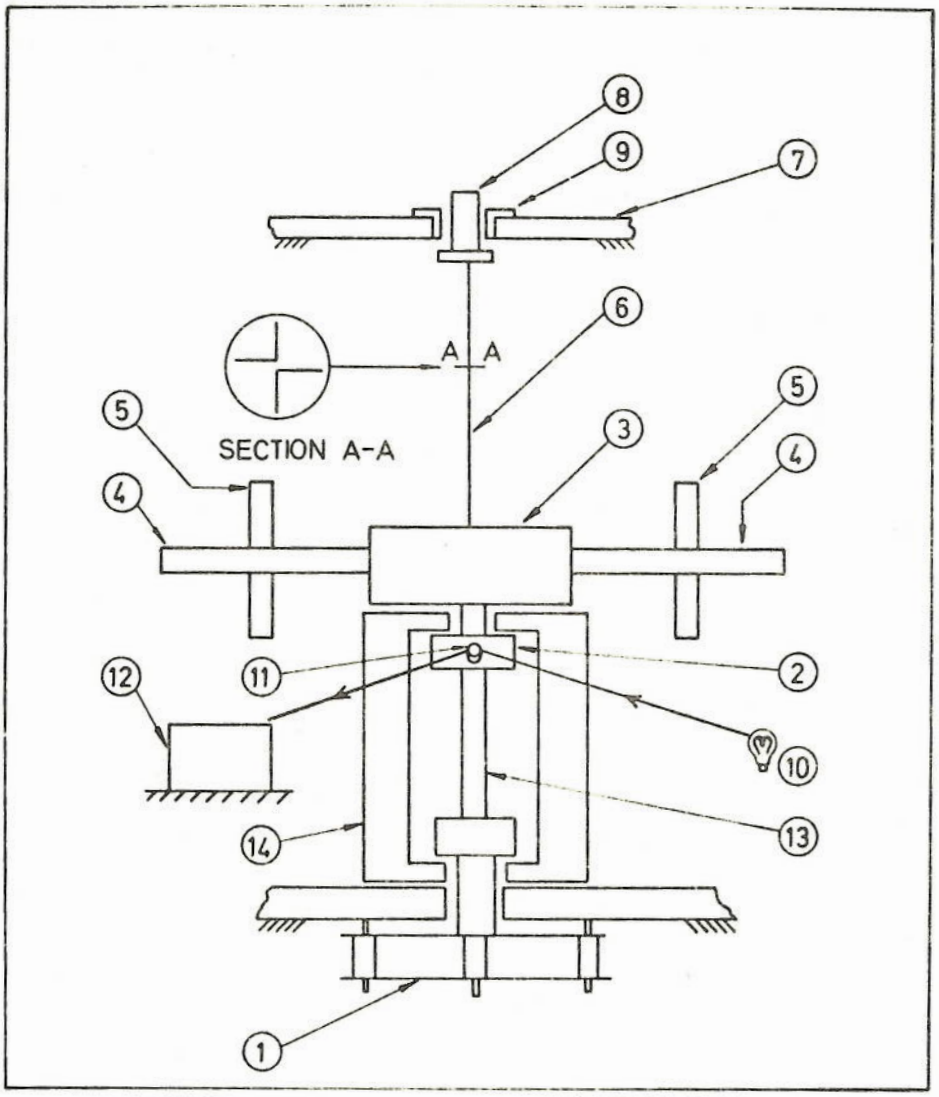

FIGURE 4·3 THE TORSION PENDULUM APPARATUS.

(1) BOTTOM CLAMP AND LINEAR BEARING ARRANGEMENT
(2) UPPER CLAMP (3) ALUMINIUM BOSS (4) INERTIA BARS
(5) INERTIA BOB (6) SUSPENSION ELEMENT (7) UPPER FIXED PLATE (8) GROUND SLIDE GUIDE (9) BUSH
(10) LIGHT SOURCE (11) MIRROR (12) GRAPHISPOT RECORDER
(13) SAMPLE (14) TEMPERATURE ENCLOSURE

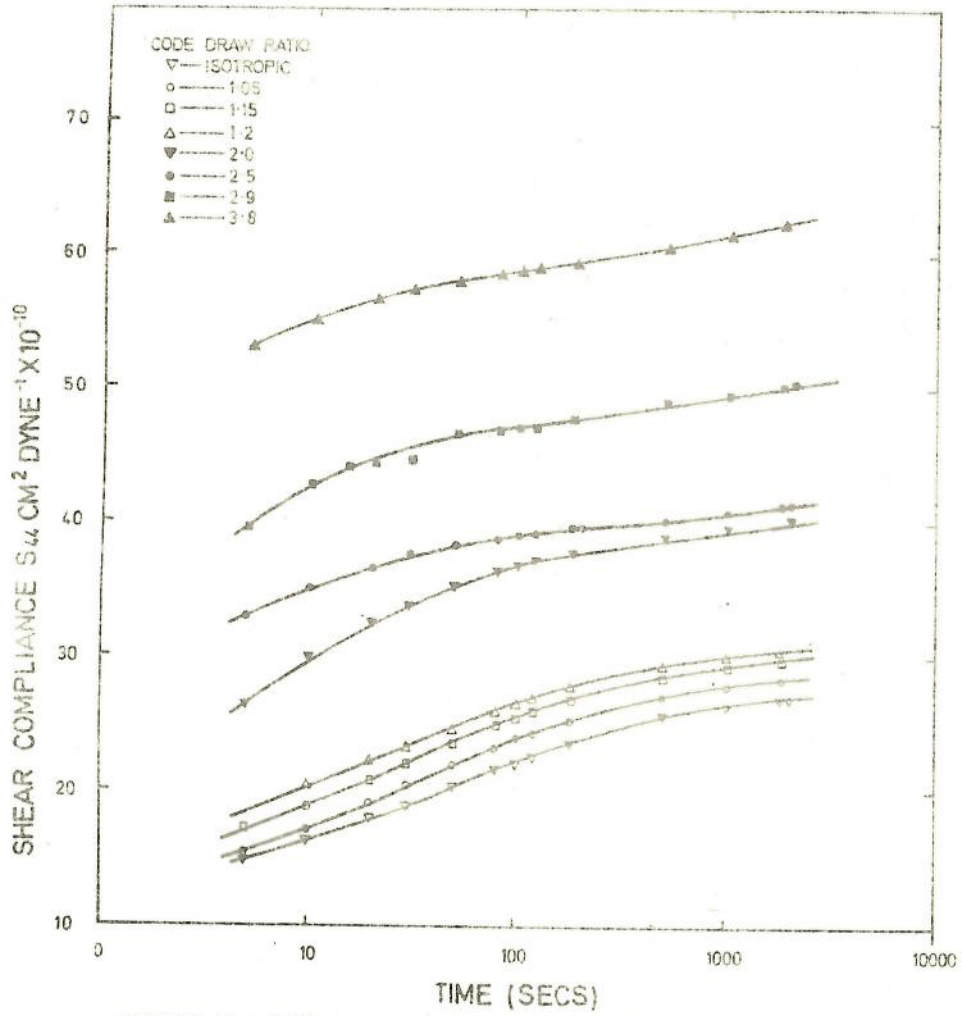

FIGURE 6·1 THE VARIATION OF THE SHEAR COMPLIANCE, $S_{44}(t)$ WITH LOG (TIME) FOR DIFFERENT DRAW RAT'OS

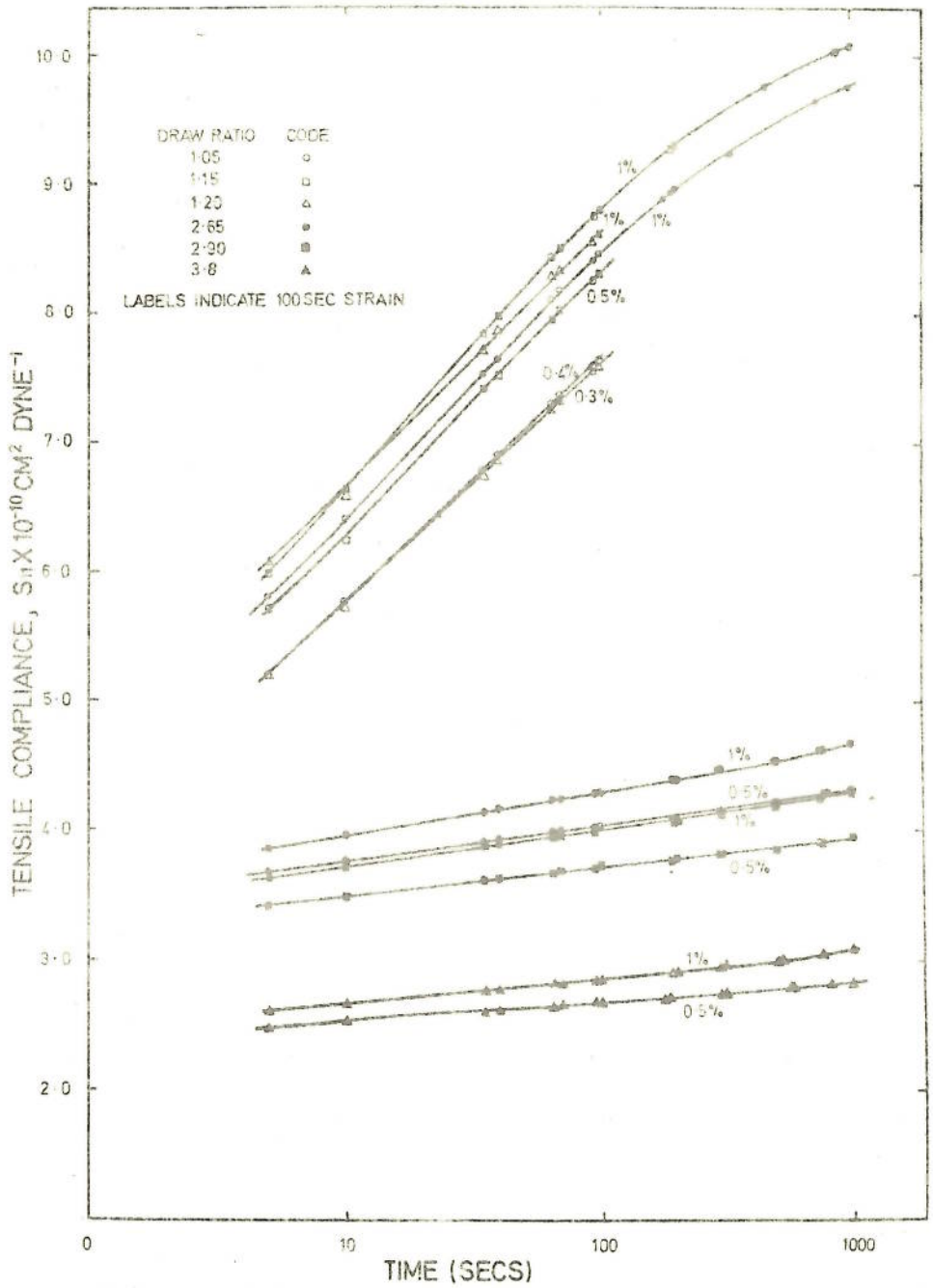

FIGURE 6·2 THE VARIATION OF THE TENSILE COMPLIANCE $S_{11}(t)$ WITH LOG (TIME) FOR DIFFERENT DRAW RATIOS AND DIFFERENT 100 SECOND STRAIN LEVELS.

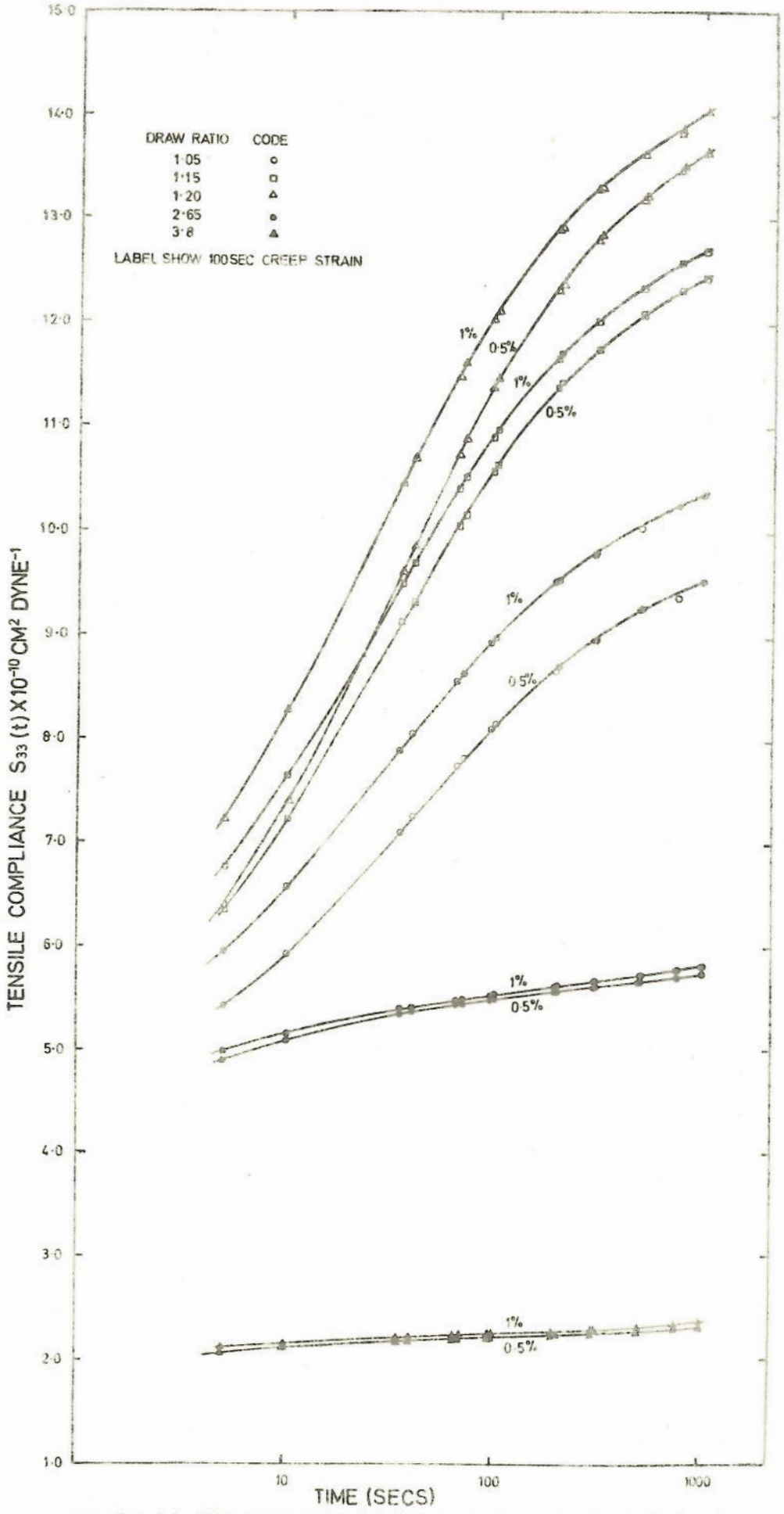

FIGURE 6·3 THE VARIATION OF THE TENSILE COMPLIANCE $S_{33}(t)$ WITH LOG(TIME) FOR DIFFERENT DRAW RATIOS AND DIFFERENT 100 SECOND STRAIN LEVELS.

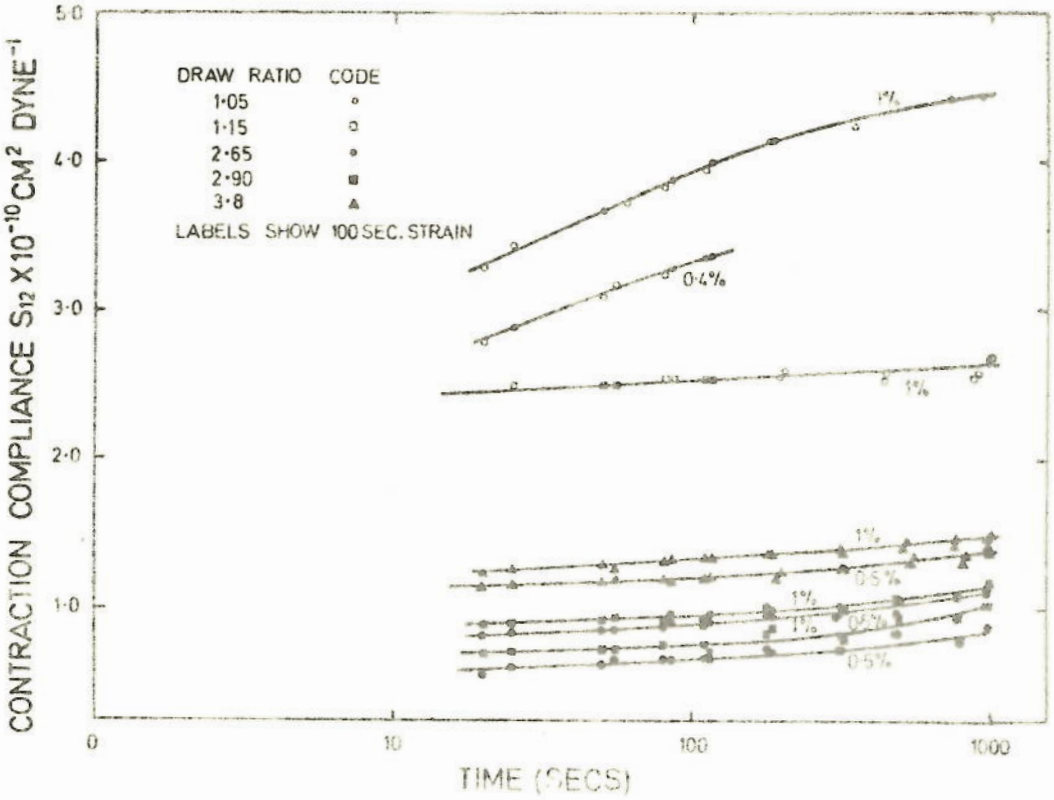

FIGURE 6.4 THE VARIATION OF THE CONTRACTION COMPLIANCE $S_{12}(t)$ V LOG (TIME) FOR DIFFERENT DRAW RATIOS AND DIFFERENT 100 SECOND STRAIN LEVELS

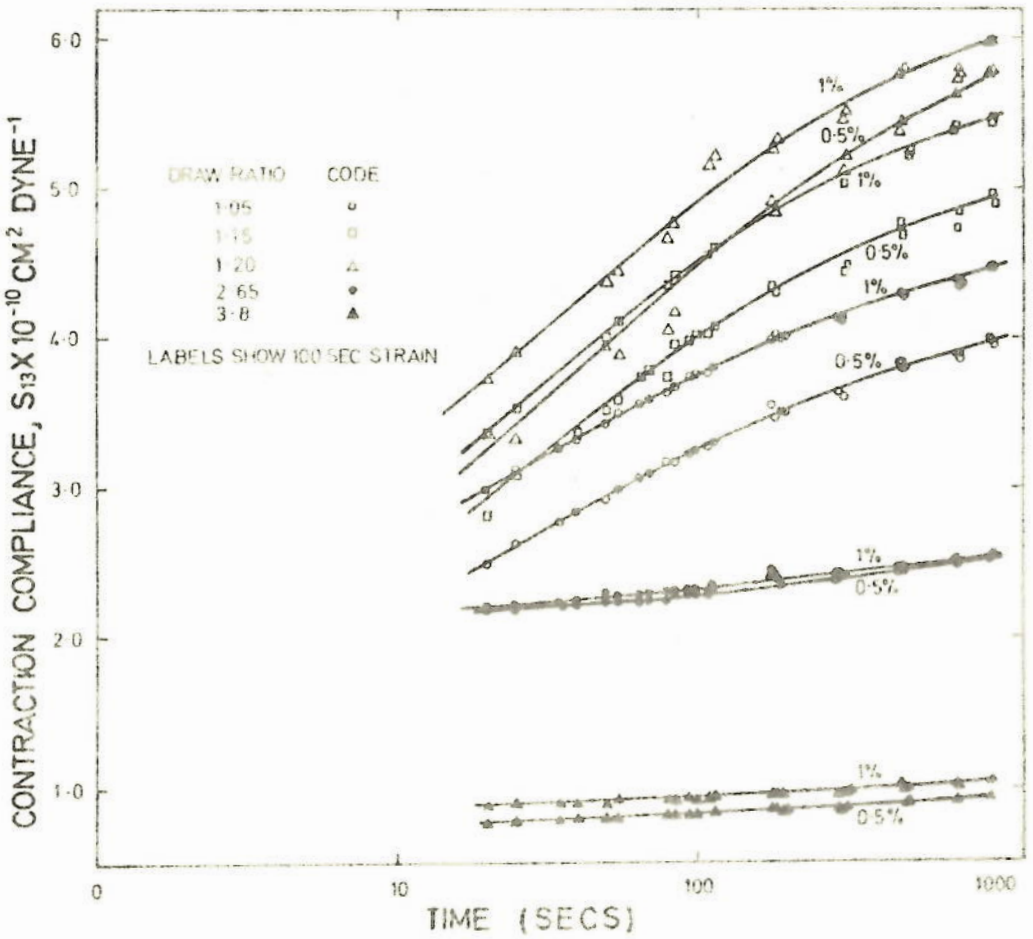

FIGURE 6·5 THE VARIATION OF THE CONTRACTION COMPLIANCE, $S_{13}(t)$, WITH LOG TIME AT DIFFERENT DRAW RATIOS AND DIFFERENT 100 SECOND STRAIN LEVELS.

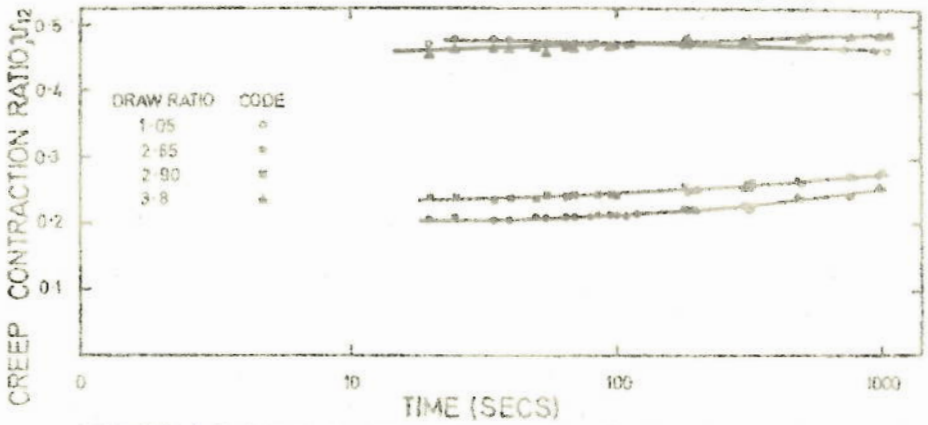

FIGURE 6.6 THE VARIATION OF CREEP CONTRACTION RATIO $\nu_{12}(t)$ WITH LOG (TIME) FOR DIFFERENT DRAW RATIOS AT 1% 100 SECOND TENSILE STRAIN.

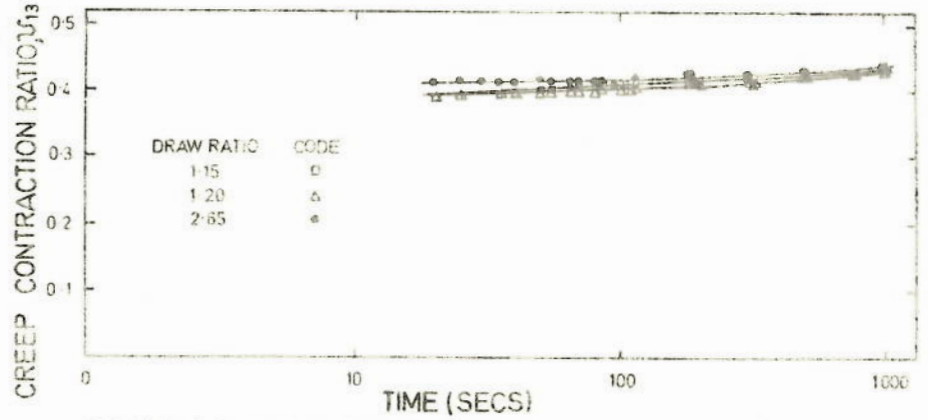

FIGURE 6·7 THE VARIATION OF CREEP CONTRACTION RATIO $\nu_{13}(t)$ WITH LOG (TIME) FOR DIFFERENT DRAW RATIOS AT 1% 100 SECOND TENSILE STRAINS.

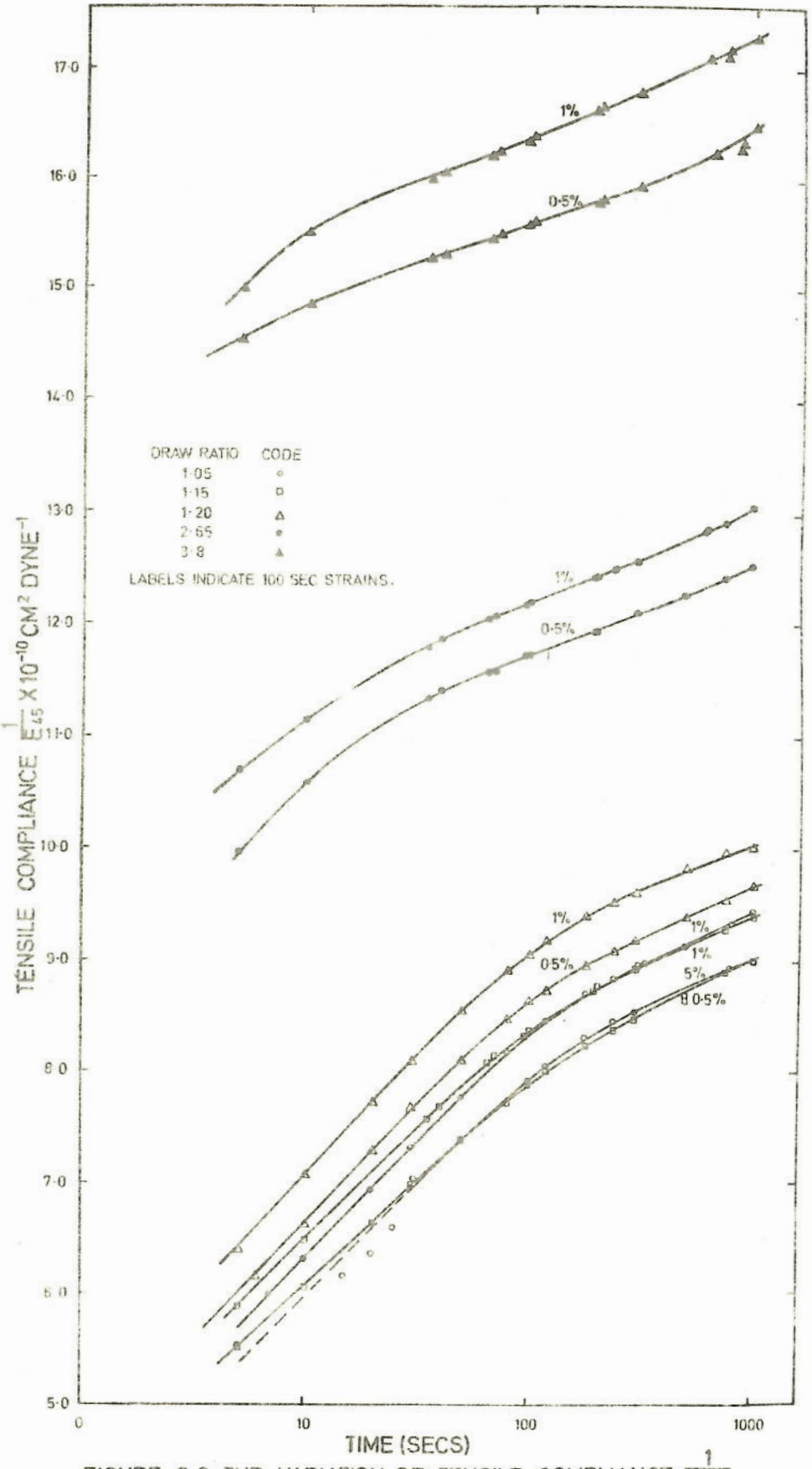

FIGURE 6·8 THE VARIATION OF TENSILE COMPLIANCE $\frac{1}{E_{45}(t)}$, WITH LOG (TIME) FOR DIFFERENT DRAW RATIOS AND DIFFERENT 100 SECOND STRAIN LEVELS

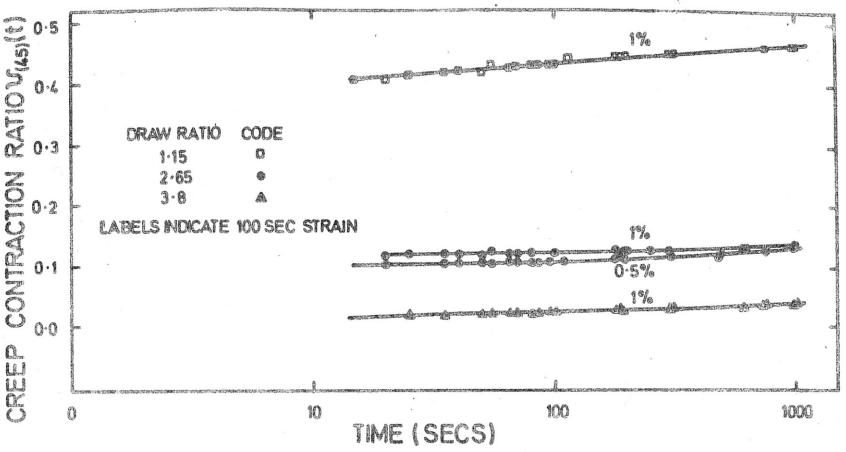

FIGURE 6·9 THE VARIATION OF CREEP CONTRACTION RATIO, $\upsilon_{45°}(t)$, WITH LOG (TIME) FOR DIFFERENT DRAW RATIOS.

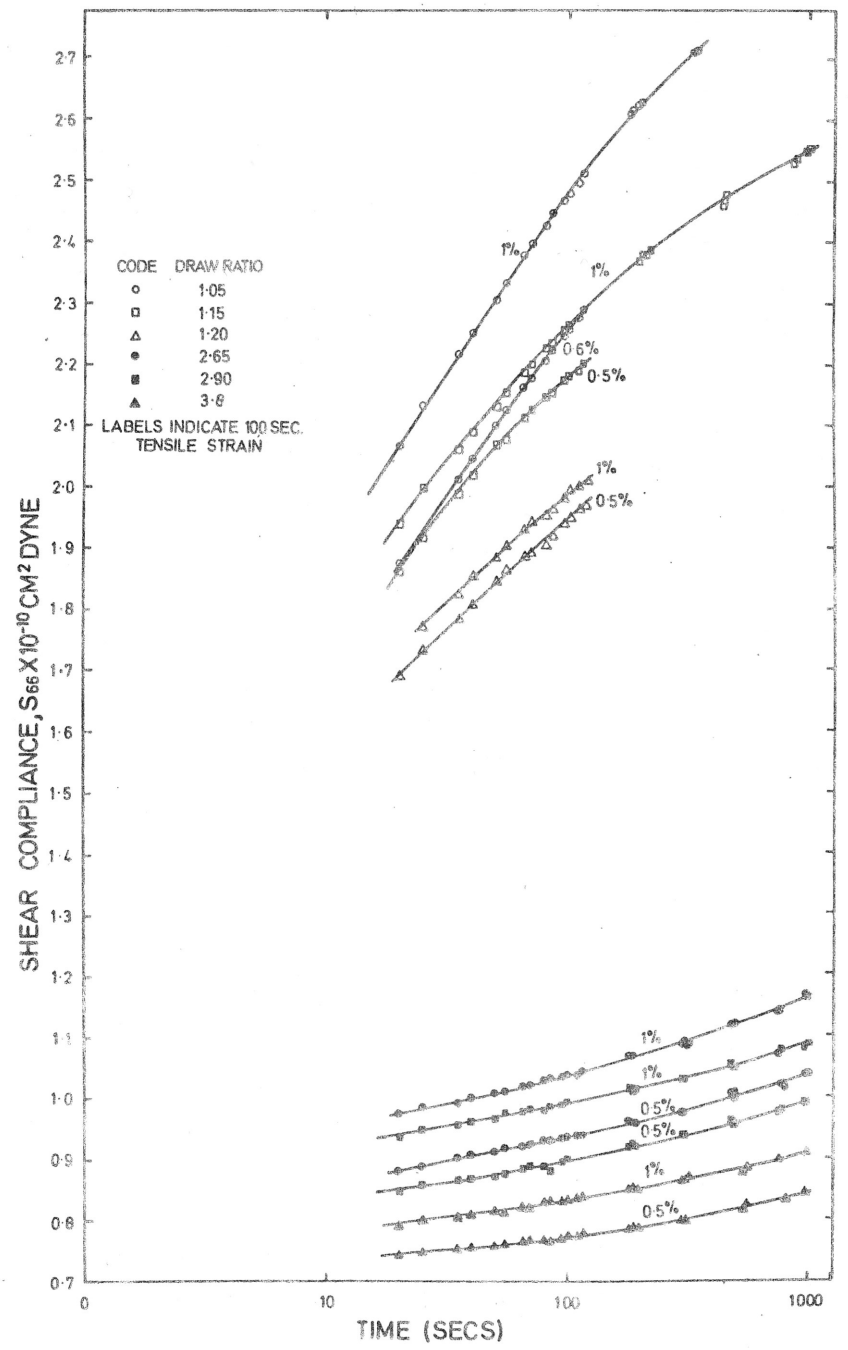

FIGURE 6·10 THE VARIATION OF CALCULATED SHEAR COMPLIANCE $S_{66}(t)$, WITH LOG (TIME) FOR DIFFERENT DRAW RATIOS AND DIFFERENT 100 SECOND STRAIN LEVELS.

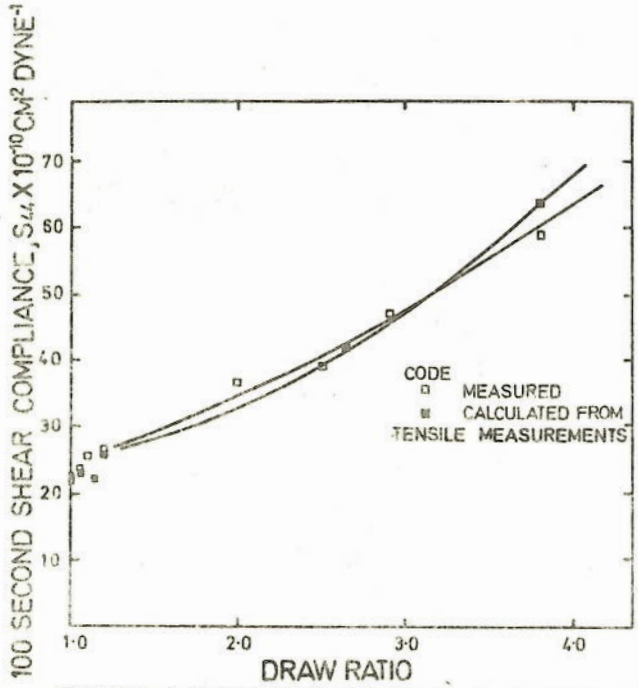

FIGURE 6·11 THE VARIATION OF MEASURED AND CALCULATED 100 SECOND SHEAR COMPLIANCE $S_{44}(t)$, WITH DRAW RATIO.

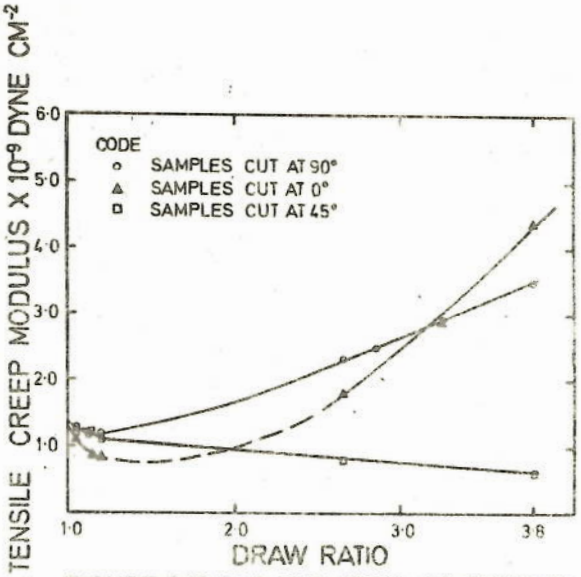

FIGURE 6.12 THE VARIATION OF TENSILE CREEP MODULI, $E_0(t)$, $E_{90}(t)$ AND $E_{45}(t)$ WITH DRAW RATIO.

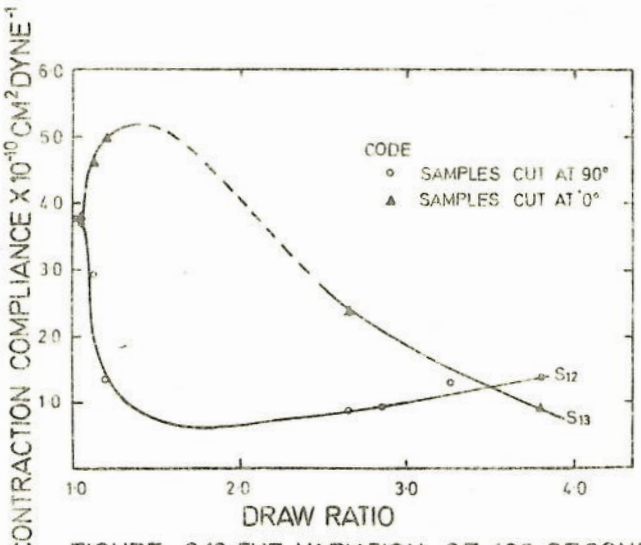

FIGURE 6.13 THE VARIATION OF 100 SECOND CONTRACTION COMPLIANCE $S_{12}(t)$ AND $S_{13}(t)$, WITH DRAW RATIO.

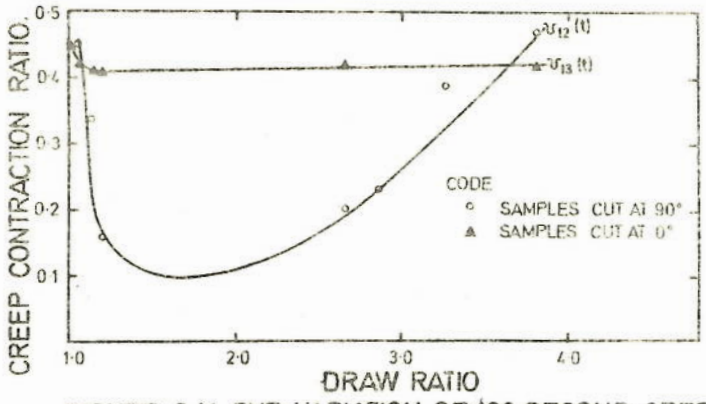

FIGURE 6·14 THE VARIATION OF 100 SECOND CREEP CONTRACTION RATIO, $\upsilon_{12}(t)$ $\upsilon_{13}(t)$ WITH DRAW RATIO

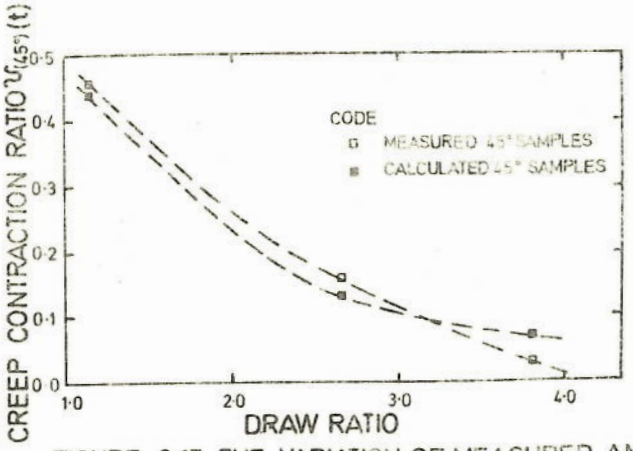

FIGURE 6·15 THE VARIATION OF MEASURED AND CALCULATED 100 SECOND CREEP CONTRACTION RATIO $\upsilon_{(45°)}(t)$ WITH DRAW RATIO.

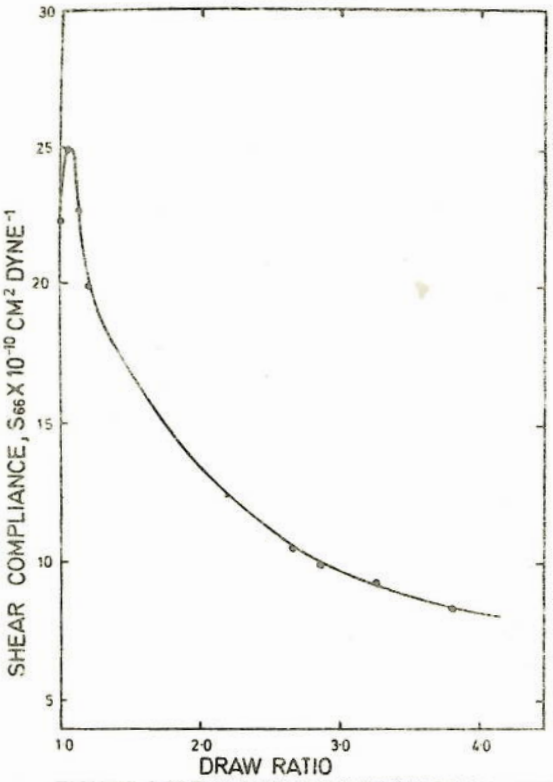

FIGURE 6·16 THE VARIATION OF THE CALCULATED 100 SECOND SHEAR COMPLIANCE, $S_{66}(t)$ WITH DRAW RATIO.

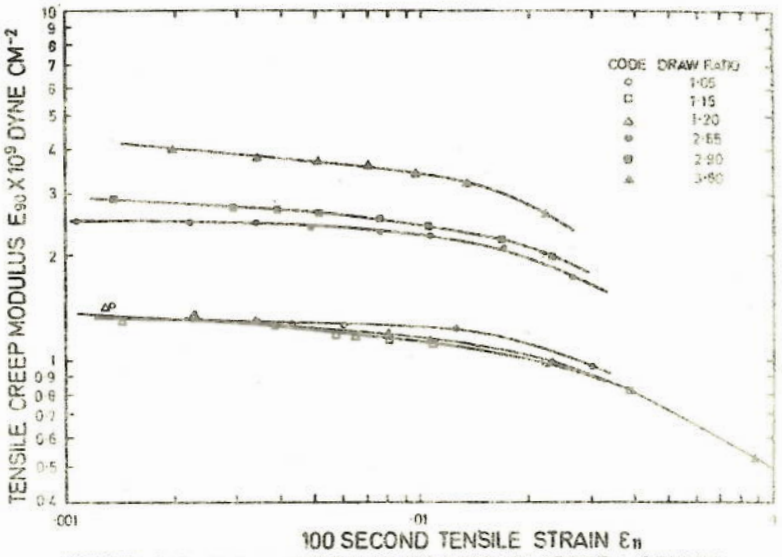

FIGURE 6·17 THE VARIATION OF 100 SECOND CREEP MODULUS $E_{90}(t)$, WITH 100 SECOND TENSILE STRAIN $\varepsilon_{11}(t)$, FOR DIFFERENT DRAW RATIOS.

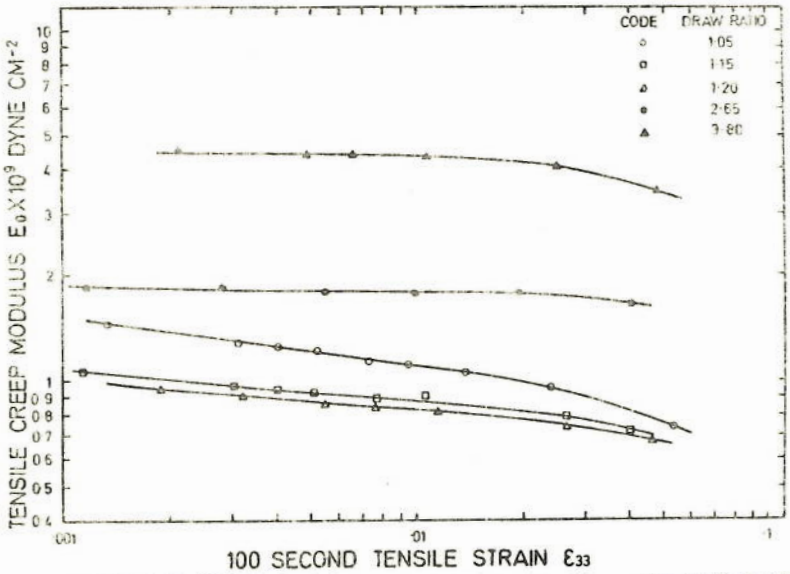

FIGURE 6·18 THE VARIATION OF 100 SECOND CREEP MODULUS $E_0(t)$ WITH 100 SECOND TENSILE STRAIN, $\varepsilon_{33}(t)$ FOR DIFFERENT DRAW RATIOS.

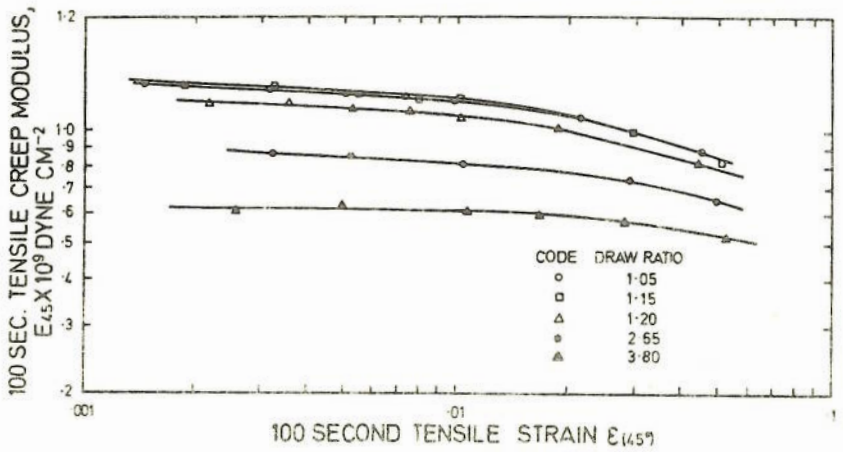

FIGURE 6·19 THE VARIATION OF 100 SECOND TENSILE CREEP MODULUS, $E_{45}(t)$, WITH 100 SECOND TENSILE STRAIN $\varepsilon_{(45°)}t$ FOR DIFFERENT DRAW RATIOS.

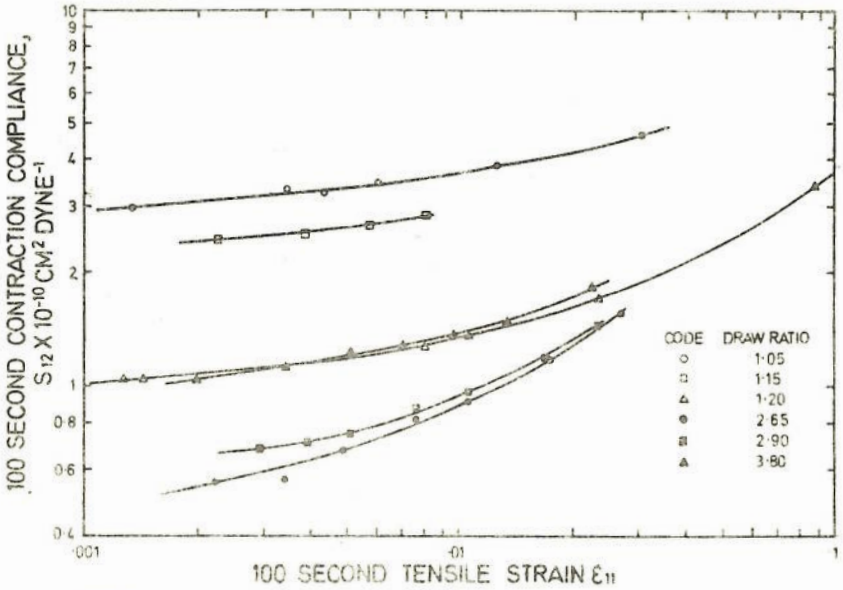

FIGURE 6·21 THE VARIATION OF 100 SECOND CONTRACTION COMPLIANCE, $S_{12}(t)$ WITH 100 SECOND TENSILE STRAIN, $\varepsilon_{11}(t)$, FOR DIFFERENT DRAW RATIOS.

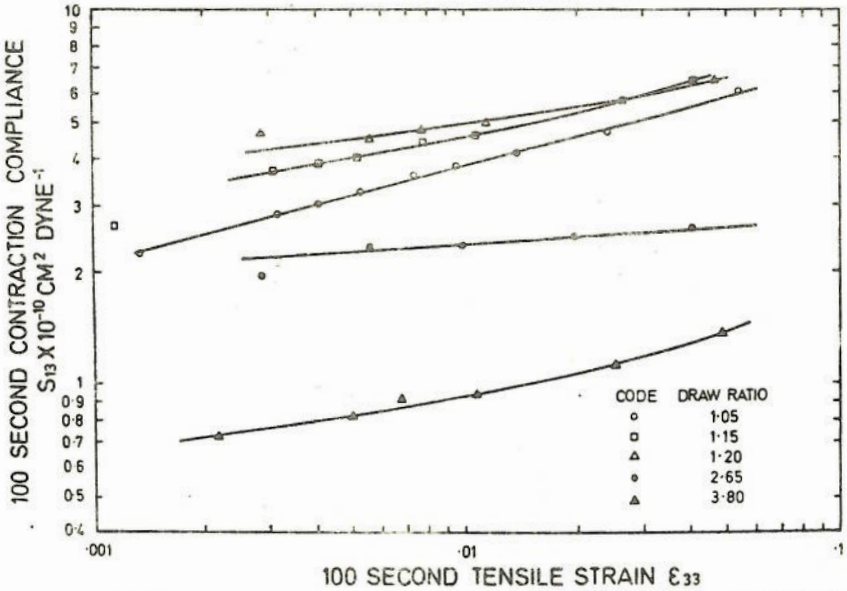

FIGURE 6·20 THE VARIATION OF 100 SECOND CONTRACTION COMPLIANCE, $S_{13}(t)$ WITH 100 SECOND TENSILE STRAIN, $S_{33}(t)$, FOR DIFFERENT DRAW RATIOS.

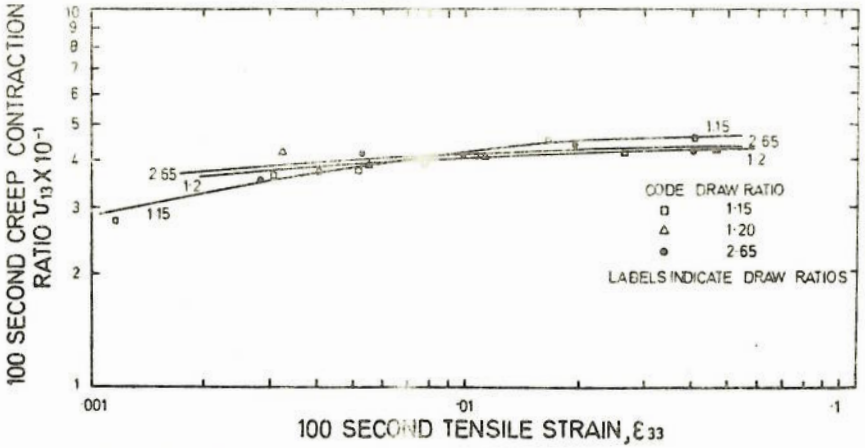

FIGURE 6·22 THE VARIATION OF 100 SECOND CREEP CONTRACTION RATIO, $U_{13}(t)$, WITH 100 SECOND TENSILE STRAIN, $\varepsilon_{33}(t)$, FOR DIFFERENT DRAW RATIOS.

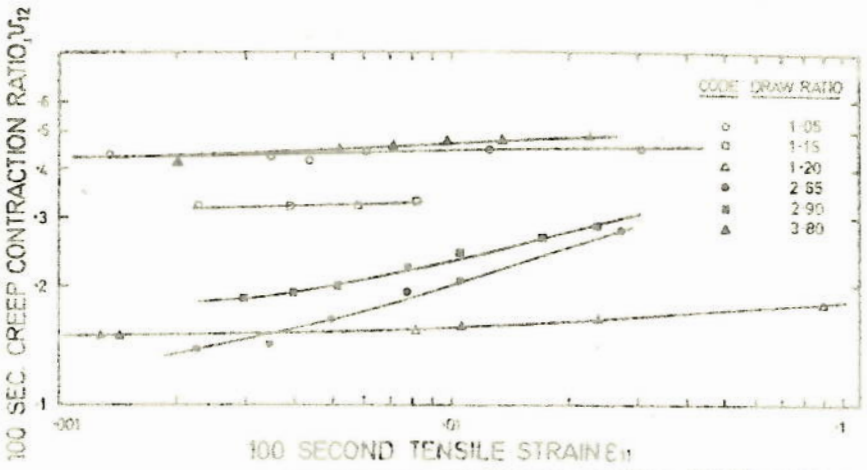

FIGURE 6.23 THE VARIATION OF 100 SECOND CREEP CONTRACTION RATIO $\nu_{12}(t)$, WITH 100 SECOND TENSILE STRAIN, $\varepsilon_{11}(t)$, FOR DIFFERENT DRAW RATIOS.

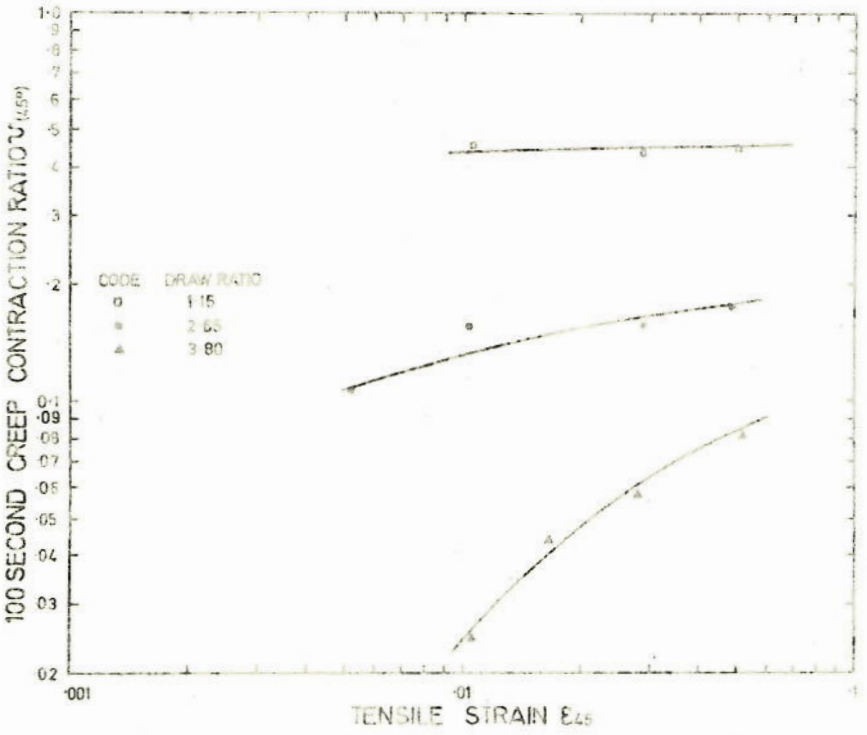

FIGURE 6.24 THE VARIATION OF 100 SECOND CREEP CONTRACTION RATIO, $\nu_{(45°)}(t)$ WITH 100 SECOND TENSILE STRAIN, $\varepsilon_{(45°)}(t)$ FOR DIFFERENT DRAW RATIOS.

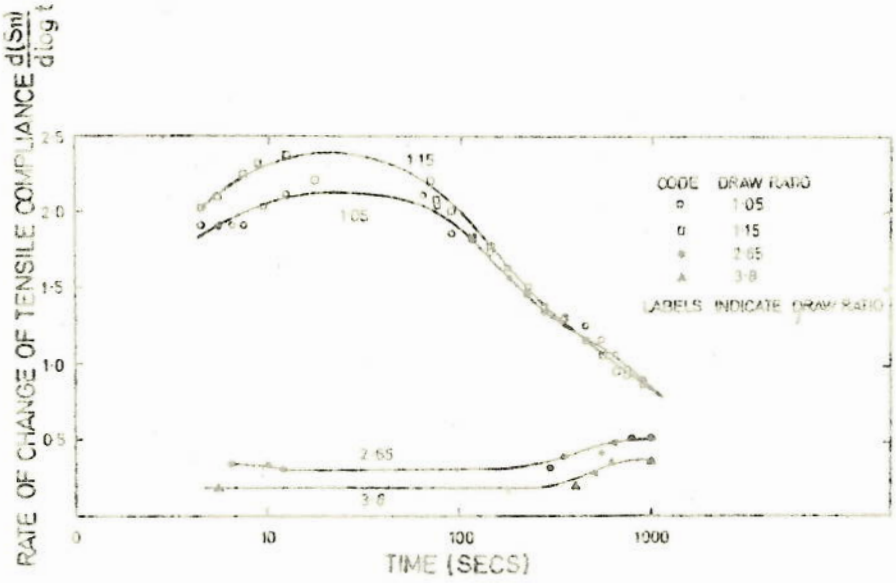

FIGURE 6.25 THE VARIATION OF RATE OF CHANGE OF TENSILE COMPLIANCE $\frac{d(S_{11}(t))}{d \log t}$ WITH LOG (TIME).

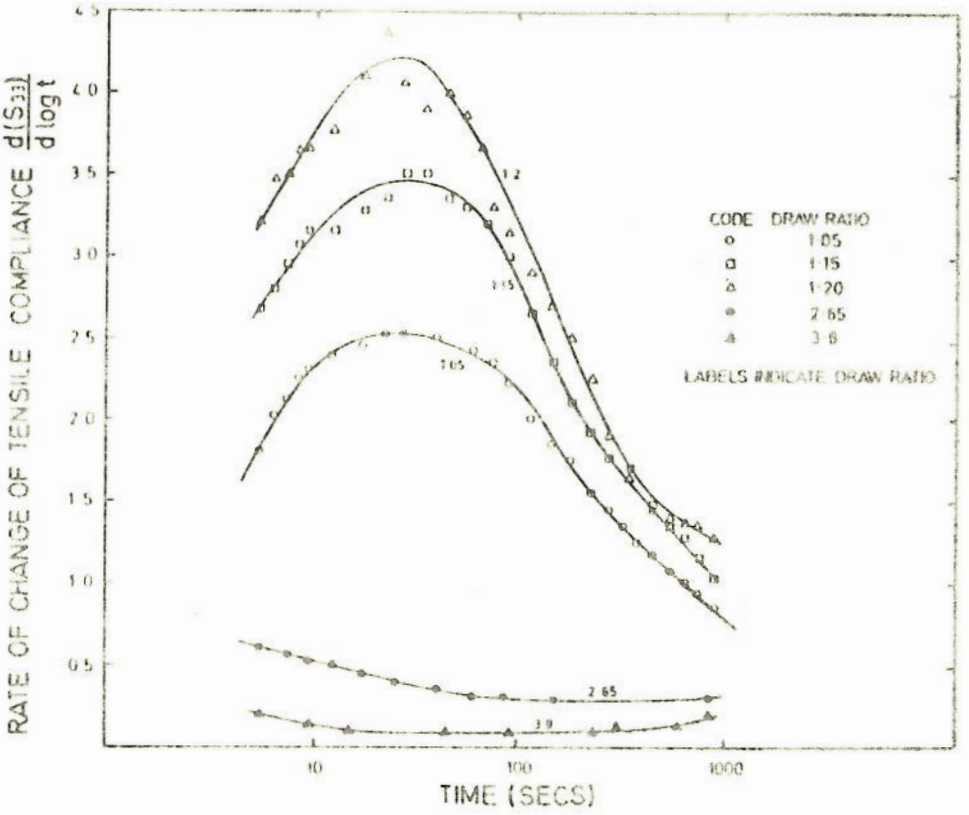

FIGURE 6.26 THE VARIATION OF THE RATE OF CHANGE OF TENSILE COMPLIANCE $\frac{d(S_{33}(t)}{d \log t}$ WITH LOG (TIME).

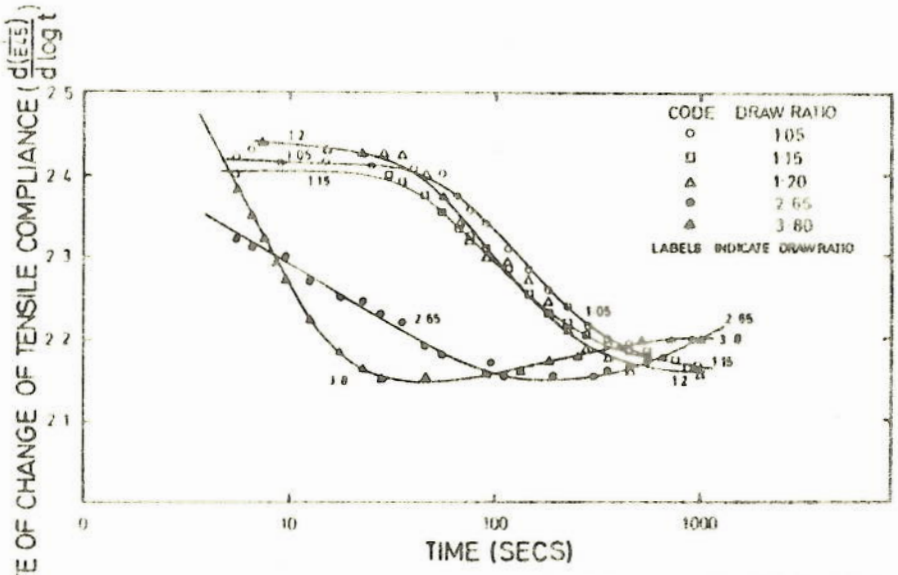

FIGURE 6.27 THE VARIATION OF RATE OF CHANGE OF TENSILE COMPLIANCE, $\frac{d(\dot{E}_{33}(t)}{d \log t}$, WITH LOG (TIME) FOR DIFFERENT DRAW RATIOS.

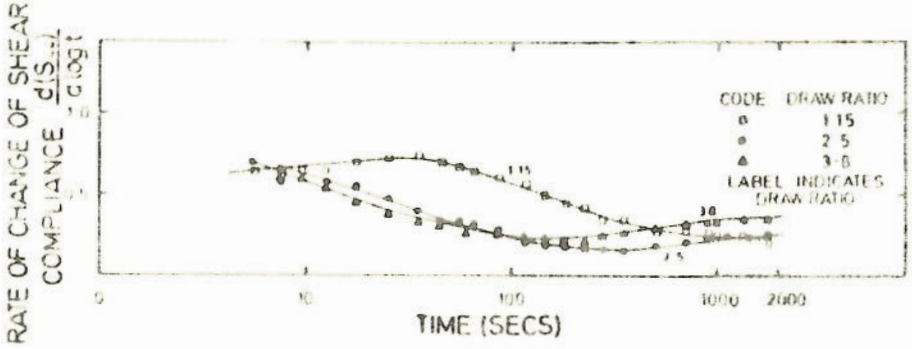

FIGURE 6.28 THE VARIATION OF THE RATE OF CHANGE OF SHEAR COMPLIANCE $\frac{d(S_{44}(t)}{d \log t}$ WITH LOG (TIME)